

Supporting Information

Heterostructured Bi₂S₃@NH₂-MIL-125(Ti) nanocomposite as a bifunctional photocatalyst for Cr(VI) reduction and rhodamine B degradation under visible light

Minghua Wang^{a,b}, Longyu Yang^b, Jinyun Yuan^b, Linghao He^{a,b}, Yingpan Song^b,
Hongzhong Zhang^a, Zhihong Zhang^{a,b*}, Shaoming Fang^{a,b*}

^a Henan Collaborative Innovation Center of Environmental Pollution Control and
Ecological Restoration;

^b Henan Provincial Key Laboratory of Surface & Interface Science, Zhengzhou
University of Light Industry, Zhengzhou, 450001, P. R. China.

*Corresponding authors:

Zhengzhou University of Light Industry, No. 136 Science Avenue, Zhengzhou,
450001, China.

Tel.: +86-37186609676

E-mail: mainzh@163.com or mingfang@zzuli.edu.cn.

Contents

S1. Synthesis of Bi_2S_3 and $\text{NH}_2\text{-MIL-125(Ti)}$

S2. XPS spectra of all samples

S3. Surface morphologies of the $\text{NH}_2\text{-MIL-125(Ti)}$ and Bi_2S_3 samples

S4. N_2 adsorption-desorption isotherms of the samples

S5. Photocatalytic activity of the samples

S6. The reusability and stability of the as-synthesized photocatalyst

S7. Mott–Schottky analysis of the as-prepared samples

S1. Synthesis of Bi₂S₃ and NH₂-MIL-125(Ti)

Bi₂S₃ was synthesized according to the previous report.¹ In typical, 1.82 g Bi(NO₃)₃·3H₂O was first dissolved into 25 mL ethylene glycol (EG) under nitrogen bubbling and obtained solution A. Meanwhile, 1.35 g Na₂S was dissolved in a mixed solvent of 10 mL EG and 20 mL deionized water under stirring for 15 min, which denoted as solution B. Then solution B was added dropwise to solution A under magnetic stirring, along with plenty of black suspended matter. Subsequently, 1.92 g carbamide and 20 mL deionized water were added to the mixture and stirred for another 30 min. The mixed solution was then transferred into a Teflon-lined stainless steel autoclave and maintained at 180 °C for 24 h. After cooling to room temperature, the precipitate was collected by vacuum filtration, and washed successively by ethanol and water for several times. Finally, the obtained products were dried under vacuum at 60 °C for obtaining the Bi₂S₃.

NH₂-MIL-125(Ti) was synthesized using a solvothermal method.^{2, 3} The H₂BDC-NH₂ (2.2 g), DMF (36 mL), methanol (4.0 mL), and Ti(OC₄H₉)₄ (2.4 mL) were mixed and dispersed with magnetic stirring for 5 mins to form a homogeneous solution. Then, the solution was poured into a Teflon-lined stainless-steel autoclave for 48 h at 150 °C. After cooling to room temperature, the obtained precipitate was separated by centrifugation, following by being washed repeatedly with DMF and methanol and dried at 60 °C overnight. As such, the NH₂-MIL-125(Ti) was obtained.

S2. XPS spectra of the samples

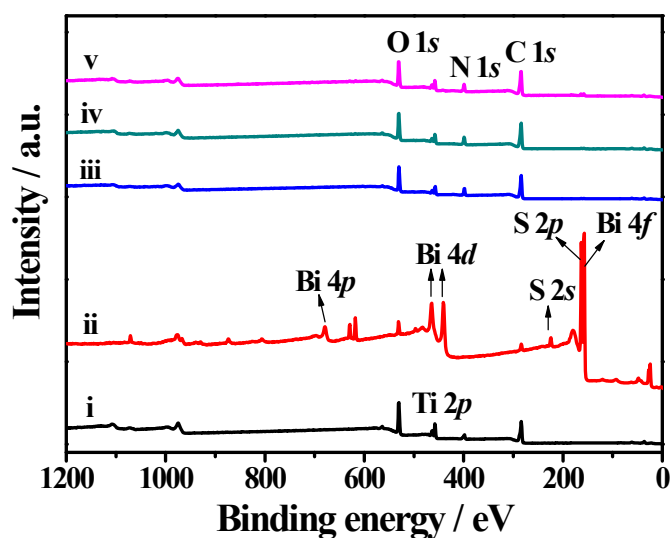


Fig. S1. XPS survey spectra of (i) NH₂-MIL-125(Ti), (ii) Bi₂S₃, (iii) Bi₂S₃@NM-10, (iv) Bi₂S₃@NM-50, and (v) Bi₂S₃@NM-100 nanocomposites.

Table S1. Atomic percentage of NH₂-MIL-125(Ti), Bi₂S₃, and Bi₂S₃@NM nanocomposites.

Samples	Atomic percentage					
	C 1s	N 1s	O 1s	Ti 2p	Bi 4f	S 2p
NH ₂ -MIL-125(Ti)	55.39	7.33	30.37	6.91	-	-
Bi ₂ S ₃	9.75	-	-	-	6.1	84.15
Bi ₂ S ₃ @NM-10	62.33	10.56	22.74	4.16	0.04	0.18
Bi ₂ S ₃ @NM-50	61.60	10.34	22.93	4.46	0.06	0.61
Bi ₂ S ₃ @NM-100	59.89	9.98	23.11	4.86	0.19	1.98

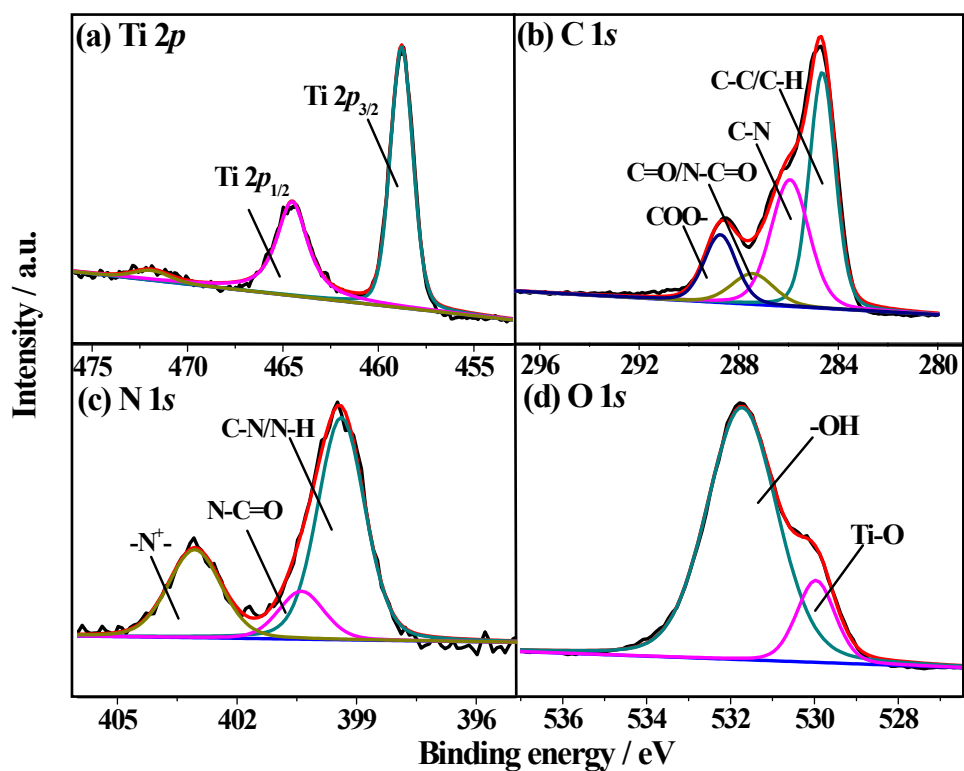


Fig. S2. (a) Ti 2*p*, (b) C 1*s*, (c) N 1*s*, and (d) O 1*s* high resolution XPS spectra of NH₂-MIL-125(Ti).

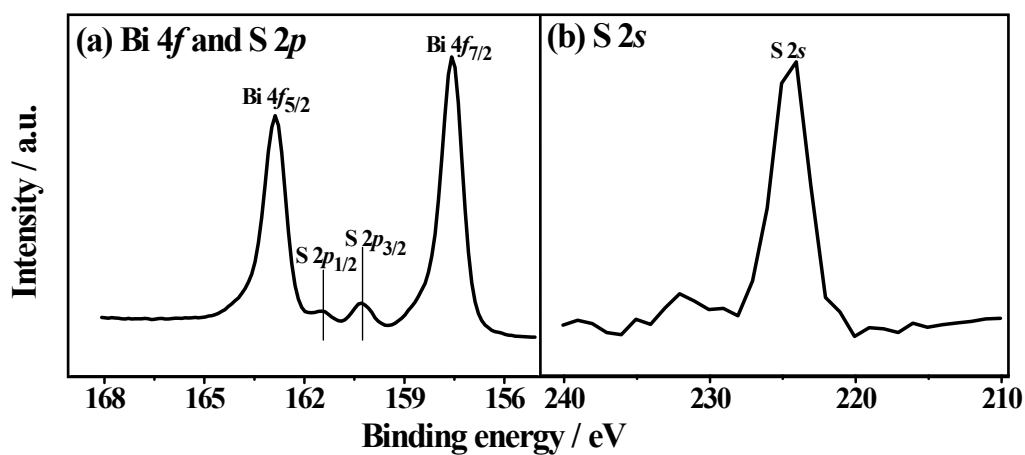


Fig. S3. (a) Bi 4*f* and S 2*p*, and (b) S 2*s* high resolution XPS spectra of Bi₂S₃.

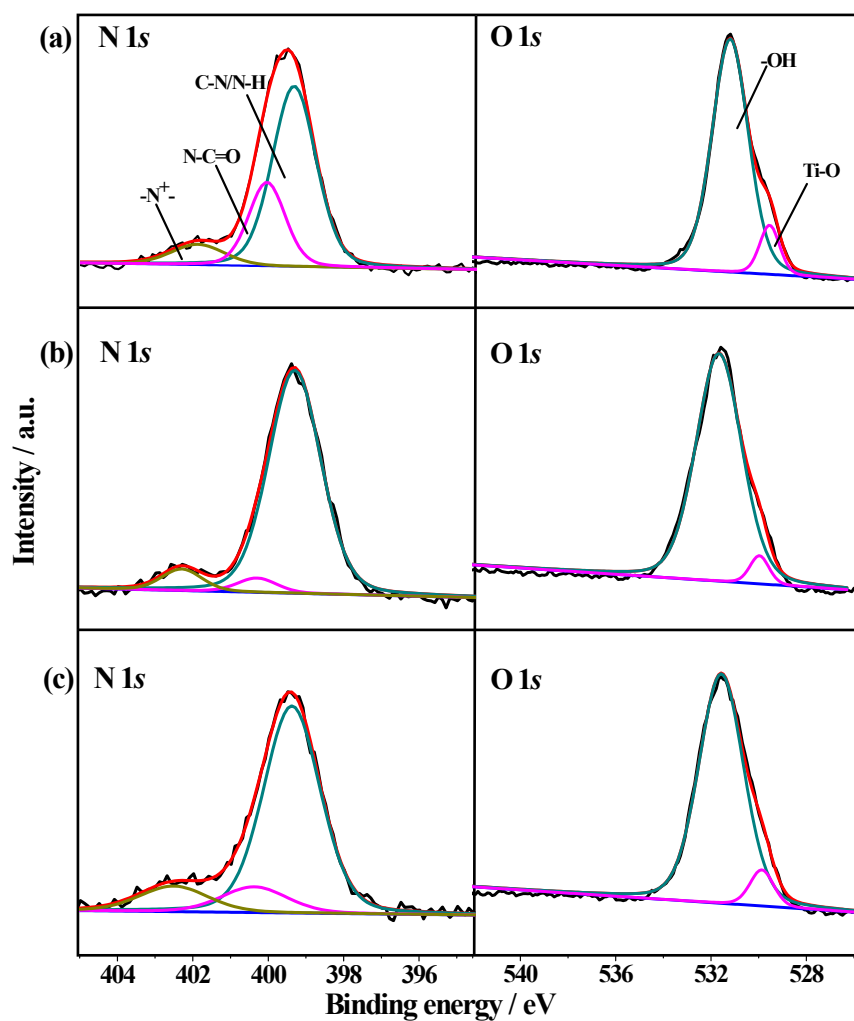


Fig. S4. N 1s and O 1s high resolution XPS spectra of (a) Bi₂S₃@NM-10, (b) Bi₂S₃@NM-50, and (c) Bi₂S₃@NM-100 nanocomposites.

S3. Surface morphologies of the $\text{NH}_2\text{-MIL-125(Ti)}$ and Bi_2S_3 samples

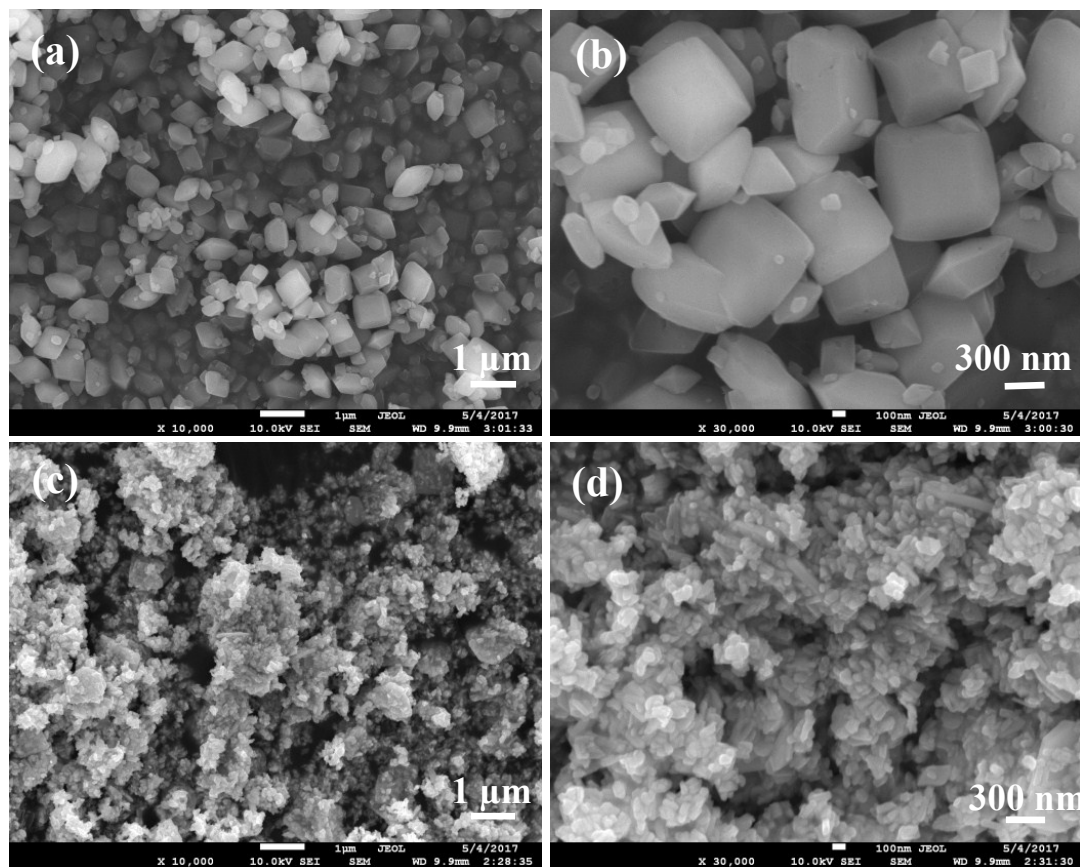


Fig. S5. Low- and high-magnification FE-SEM images of (a, b) $\text{NH}_2\text{-MIL-125(Ti)}$ and (c, d) Bi_2S_3 .

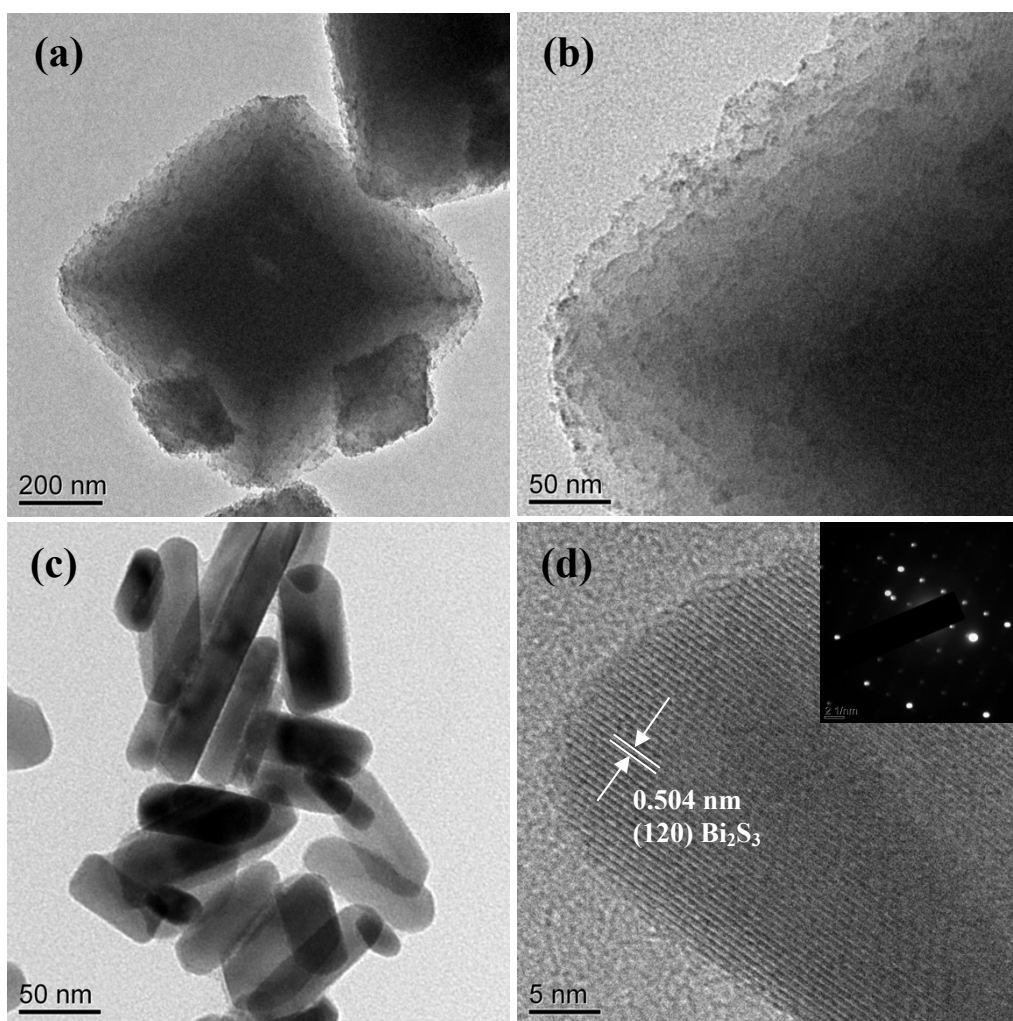
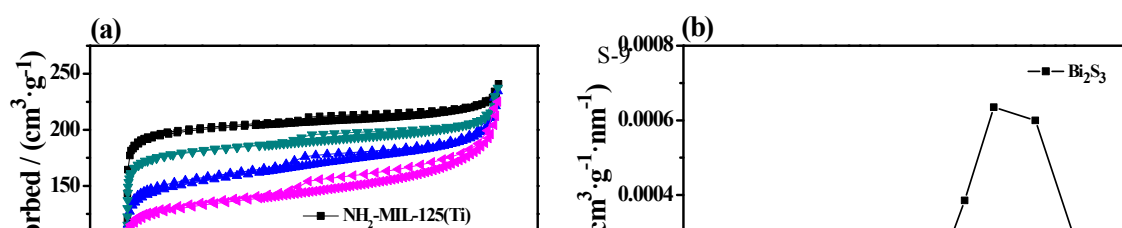


Fig. S6. (a, b) TEM images of NH₂-MIL-125(Ti) and (c, d) TEM and HR-TEM images of Bi₂S₃ (the inset in (d) is the corresponding SAED pattern).

S4. Nitrogen adsorption-desorption isotherms of the samples

To evaluate the pore structures and specific surface areas, N₂ adsorption–desorption measurements of all samples were performed, as shown in **Figure S7**. The NH₂-MIL-125(Ti) sample illustrated type I isotherms at 77 K with no hysteresis, indicating its typical microporous structure. The Bi₂S₃ exhibited type IV isotherms with a hysteresis loop in the higher relative pressure (P/P_0 , 0.9–1.0) range, which implies the presence of capillary condensation in the mesoporous and macroporous. N₂ adsorption-desorption isotherms of Bi₂S₃@NM samples exhibit hybrid type I/IV isotherms with hysteresis loop at $P/P_0 = 0.45–1.0$, confirming the presence of both of micropores and mesopores.⁴ It illustrated that the specific surface area of NH₂-MIL-125(Ti), Bi₂S₃@NM-10, Bi₂S₃@NM-50, and Bi₂S₃@NM-100 were determined to be 622.9, 485.7, 560.9, and 416.7 m²·g⁻¹ using Brunauer–Emmett–Teller (BET) method. The pore size distributions were obtained from the Barrett–Joyner–Halenda (BJH) method and Horvath-Kawazoe (HK) method. An extremely little specific surface area was observed for Bi₂S₃, only 12.5 m²·g⁻¹, with a wide distribution centered around 40-65 nm (**Figure S7b**). The NH₂-MIL-125(Ti) and Bi₂S₃@NM samples (**Figure S7c-d**) revealed narrow distributions centered at 0.5–1 nm and narrow distributions ranged from 3–5 nm, which were associated with the microporous and mesoporous structure.



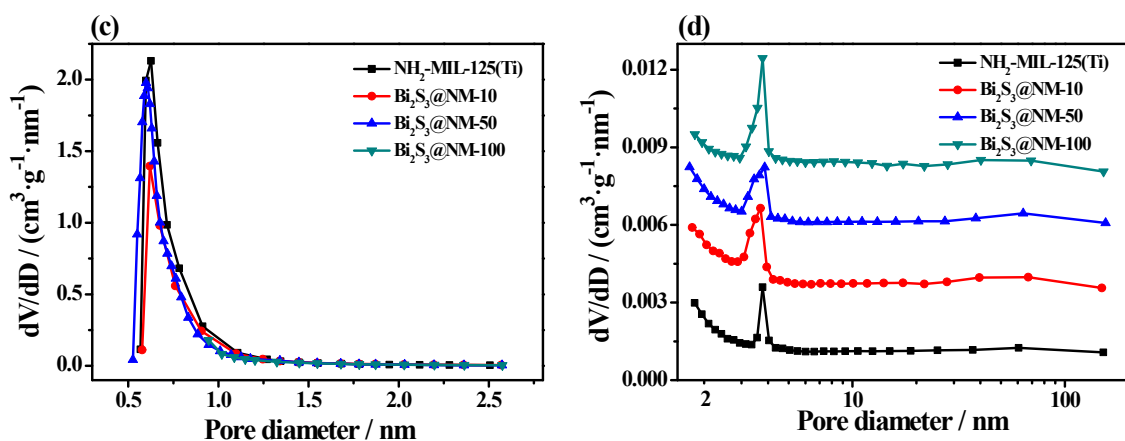


Fig. S7. (a) Nitrogen adsorption–desorption isotherms of $\text{NH}_2\text{-MIL-125(Ti)}$, Bi_2S_3 , and $\text{Bi}_2\text{S}_3@\text{NM}$ nanocomposites. (b) Barrett-Joyner-Halenda (BJH) mesopore size distributions of Bi_2S_3 . (c) Horvath-Kawazoe (HK) micropore size distributions and (d) Barrett-Joyner-Halenda (BJH) mesopore size distributions of $\text{NH}_2\text{-MIL-125(Ti)}$ and $\text{Bi}_2\text{S}_3 @\text{NM}$ nanocomposites.

S5. Photocatalytic activity of the samples

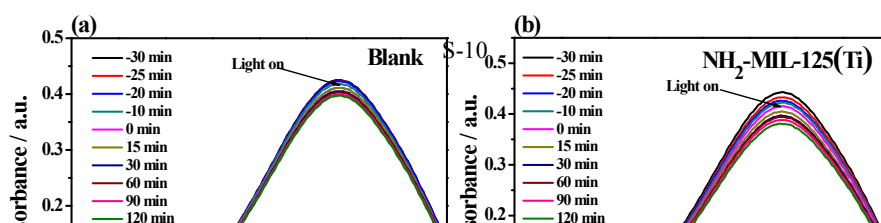


Fig. S8. UV-vis absorption spectra for reduction of Cr (VI) with (a) blank, (b) NH₂-MIL-125(Ti), (c) Bi₂S₃, (d) Bi₂S₃@NM-10, (e) Bi₂S₃@NM-50, and (f) Bi₂S₃@NM-100 catalysts. (g) Reaction rate constant (*k*) of various samples (initial concentration of Cr(VI): 10 mg·L⁻¹, photocatalyst dosage: 100 mg·L⁻¹, pH = 7.0).

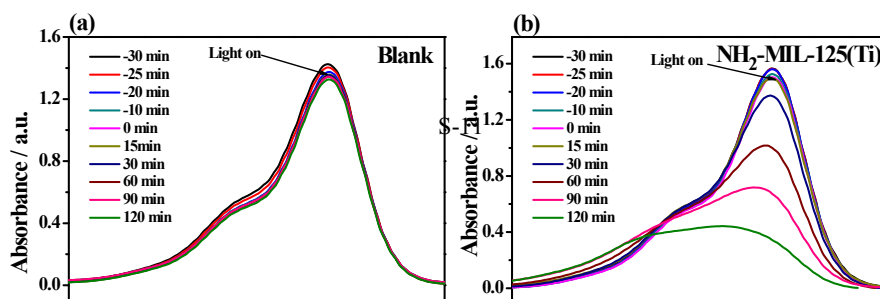


Fig. S9. UV-vis absorption spectra for degradation of RhB with (a) blank, (b) NH₂-MIL-125(Ti), (c) Bi₂S₃, (d) Bi₂S₃@NM-10, (e) Bi₂S₃@NM-50, and (f) Bi₂S₃@NM-100 catalysts. (g) reaction rate constant (*k*) of various samples (initial concentration of RhB: 20 mg·L⁻¹, photocatalyst dosage: 100 mg·L⁻¹, pH = 7.0).

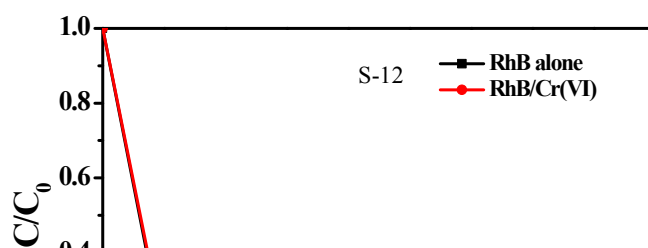


Fig. S10. Photocatalytic degradation of RhB with and without of Cr(VI) using the $\text{Bi}_2\text{S}_3@\text{NM-100}$ sample (initial concentration of RhB: $5 \text{ mg}\cdot\text{L}^{-1}$, Cr(VI): $10 \text{ mg}\cdot\text{L}^{-1}$, photocatalyst dosage: $200 \text{ mg}\cdot\text{L}^{-1}$, pH = 3.0).

S6. The reusability and stability of the photocatalyst

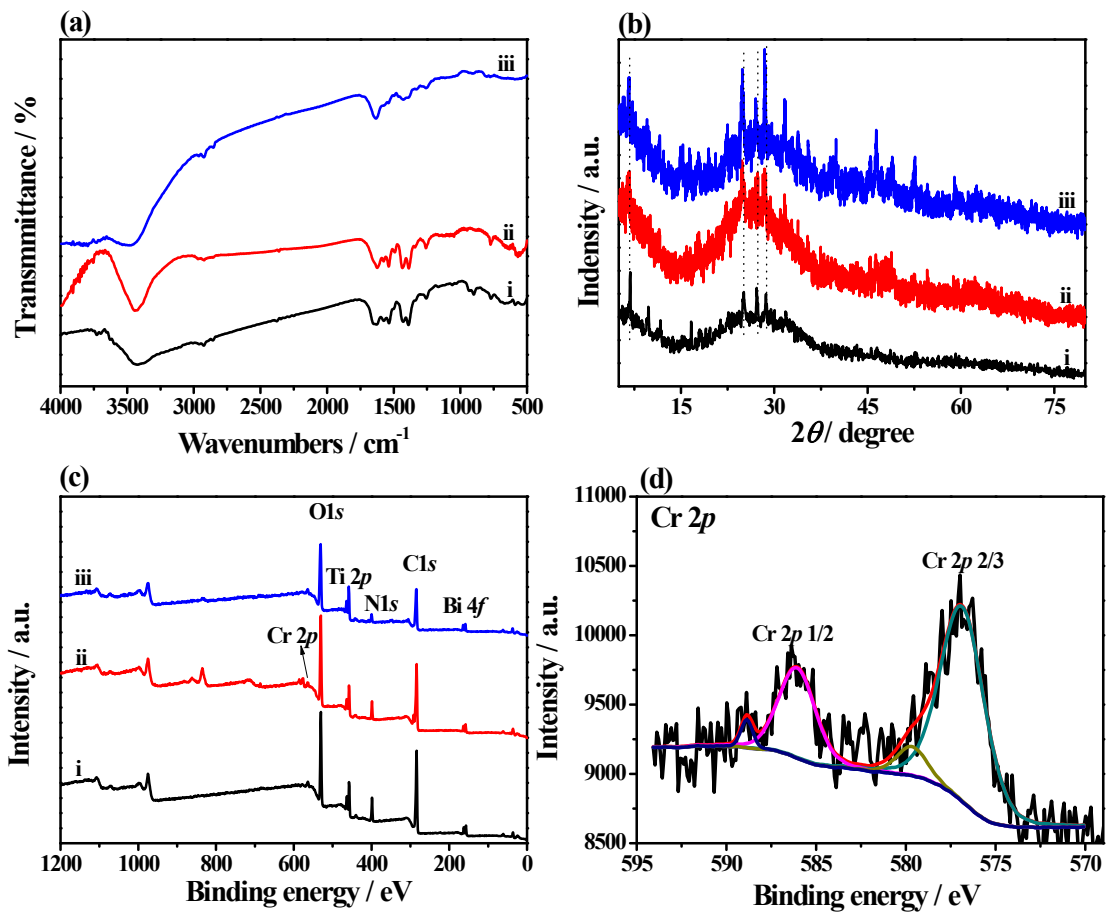


Fig. S11. (a) FT-IR spectra, (b) XRD patterns, (c) XPS survey spectra and of the (i) pristine $\text{Bi}_2\text{S}_3@\text{NM-100}$, and recycled sample after (ii) Cr(VI) reduction and (iii) RhB degradation. (d) High-resolution XPS spectrum of Cr 2p for the recycled $\text{Bi}_2\text{S}_3@\text{NM-100}$ after photocatalytic reduction of Cr(VI).

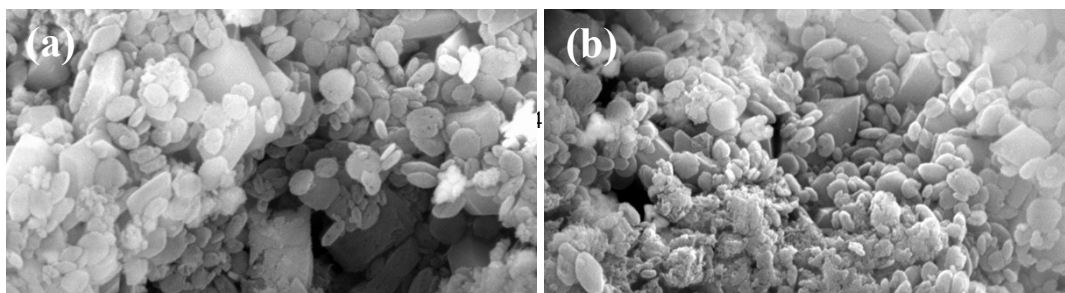


Fig. S12. FE-SEM images of the recycled $\text{Bi}_2\text{S}_3@\text{NM-100}$ after (a) Cr(VI) reduction and (b) RhB degradation.

S7. Mott-Schottky analysis



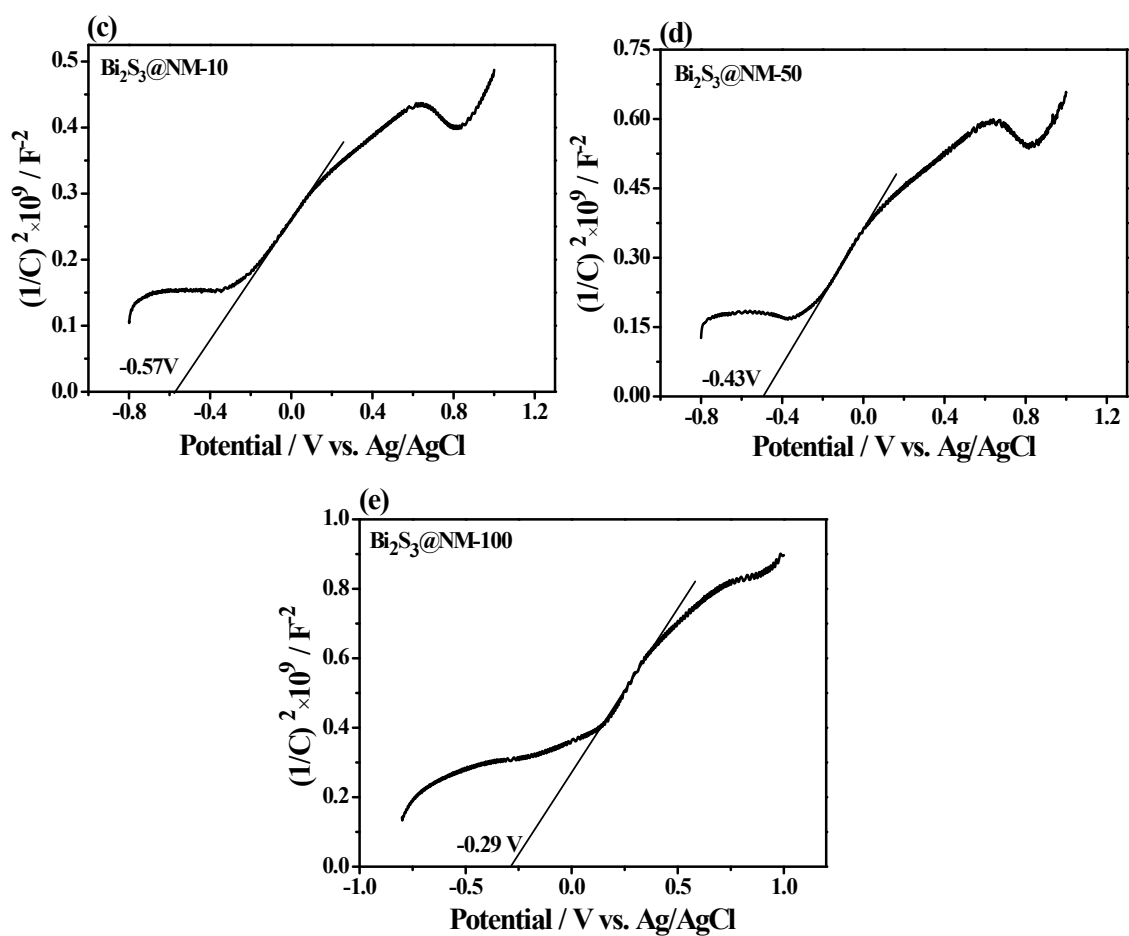


Fig. S13. Mott-Schottky plots of (a) $\text{NH}_2\text{-MIL-125(Ti)}$, (b) Bi_2S_3 , (c) $\text{Bi}_2\text{S}_3@\text{NM-10}$, (d) $\text{Bi}_2\text{S}_3@\text{NM-50}$, and (e) $\text{Bi}_2\text{S}_3@\text{NM-100}$ nanocomposites measured in 0.5 M Na_2SO_4 aqueous solution at a frequency of 100 Hz in the dark.

Table S2. The values of flat-band, conduction band, valence band, and E_g for various

samples.

Samples	Flat band (V vs. Ag/AgCl)	Flat band (V vs. NHE)	Conduction band (V vs. NHE)	Valence band (V vs. NHE)	E_g (eV)
NH ₂ -MIL- 125(Ti)	-0.70	-0.49	-0.59	2.09	2.68
Bi ₂ S ₃	-0.07	0.14	0.04	1.36	1.32
Bi ₂ S ₃ @NM-10	-0.57	-0.36	-0.46	2.20	2.66
Bi ₂ S ₃ @NM-50	-0.43	-0.22	-0.32	2.32	2.64
Bi ₂ S ₃ @NM-100	-0.29	-0.08	-0.18	2.41	2.59

References:

- 1 Z. Ge, B. Zhang, Z. Yu and B. Jiang, *Crystengcomm*, 2012, **14**, 2283-2288.
- 2 M. Dan-Hardi, C. Serre, T. Frot, L. Rozes, G. Maurin, C. Sanchez and G. Férey, *J. Am. Chem. Soc.*, 2009, **131**, 10857-10859.
- 3 Y. Fu, D. Sun, Y. Chen, R. Huang, Z. Ding, X. Fu and Z. Li, *Angew. Chem.*, 2012, **124**, 3420-3423.
- 4 Z. H. Rada, H. R. Abid, J. Shang, Y. He, P. Webley, S. Liu, H. Sun and S. Wang, *Fuel*, 2015, **160**, 318-327.